

1 **Separation of an upwelling current bounding the Juan
2 de Fuca Eddy**

3 **Jody M. Klymak^{1,2}, Susan E. Allen^{3,4}, Stephanie Waterman³**

4 ¹School of Earth and Ocean Sciences, University of Victoria, BC, Canada

5 ²Department of Physics & Astronomy, University of Victoria, BC, Canada

6 ³Department of Earth, Ocean and Atmospheric Sciences, University of British Columbia, Vancouver, BC,

7 Canada

8 ⁴Institute of Applied Mathematics, University of British Columbia, Vancouver, BC, Canada

9 **Key Points:**

- 10 • The shelf break current along Vancouver Island separates downstream of a submarine
11 bank.
- 12 • Offshore water is drawn onto the shelf and forms a sharp semi-persistent front with
13 the Juan de Fuca Eddy.
- 14 • The Eddy shows evidence of long residence times, and little evidence of deep-water
15 origin.

16 **Abstract**

17 Comprehensive water column observations of temperature, salinity, and oxygen on
 18 the productive southern Vancouver Island shelf offer a unique characterization of processes
 19 affecting exchange on the shelf. A semi-permanent cyclonic recirculation (the Juan de
 20 Fuca Eddy) occupies the region in the lee of a bank where the shelf widens abruptly. The
 21 observations indicate that the water in this Eddy is a mixture of offshore water and water
 22 from a buoyant coastal current. This water is well-mixed along a mixing line in temperature-
 23 salinity space, though it retains stratification, and is either rapidly mixed (high mixing rate
 24 κ), or has a long residence time (large τ), such that the mixing length $(\kappa\tau)^{1/2} \sim 50 - 100$ m. There is a sharp temperature-salinity front on the offshore side of this well-mixed
 25 water. The front is no more than 1-km wide, and has no sign of instabilities. Previous work
 26 had hypothesized the role of a spur canyon incising the shelf in feeding water to the Eddy;
 27 little evidence of this was found in the observations, however, these were collected during
 28 a relaxation and reversal of upwelling winds, which may have slowed the flow of water into
 29 the Eddy. Tidally resolved observations in the spur canyon also show very strong hydraulic
 30 flows in the cross-canyon direction accompanied by very high localized mixing rates in 50-m
 31 hydraulic jumps, possibly exceeding $\kappa \sim 1 \text{ m}^2\text{s}^{-2}$.
 32

33 Upstream of the Eddy, there is an along-shelf current flowing equatorward with partially
 34 mixed water properties compared to the well-mixed water in the Eddy. The shelf
 35 current was observed to separate from the shelf in the lee of a bank, and was replaced by a
 36 distinct offshore water mass. The separation event can be seen in sea-surface temperatures
 37 in satellite images as a tongue of water that is ejected offshore. The cause of this offshore
 38 separation event is not determined, but possibly is catalyzed by separation of the current
 39 from the abrupt underwater bank at the poleward end of the study region.

40 **Plain Language Summary**

41 The southern Vancouver Island continental shelf is very biologically productive due to
 42 high nutrient input from the Strait of Juan de Fuca and Salish Sea estuarine system and
 43 substantial cross-shelf transport due to the complicated topography. The estuarine water
 44 flows poleward, hugging the coast as the Vancouver Island Coastal Current and, in the
 45 summer, shelf water flows equatorward. Trapped between these two currents is the Juan de
 46 Fuca Eddy, a stagnant region of water that occupies the shelf where it abruptly widens just
 47 north of the Strait of Juan de Fuca.

48 Here we present intensive sampling of the Juan de Fuca Eddy region. The observations
 49 show that below the surface mixed layer, the water in the Eddy is low in oxygen, and has
 50 undergone substantial vertical and lateral mixing. In contrast to previous literature we find
 51 that the low oxygen in the eddy is likely because of respiration rather than being pulled
 52 from low-oxygen water in the California Undercurrent.

53 The observations also show a remarkable flow separation of the equatorward shelf
 54 current. The current is seen to detach and is pushed offshore. Such events are readily
 55 seen in satellite imagery, but our observations indicate that the separation extends the
 56 depth of the water column on the shelf, and that this separation may be partially driven
 57 by the local bathymetry. The separation is a very strong cross-shelf exchange event, and
 58 likely transports substantial nutrient-rich coastal water offshore to drive productivity in the
 59 deeper ocean adjacent to the continental slope.

60 **1 Introduction**

61 Cross-shelf exchange is important to the health and productivity of continental shelf
 62 regions, allowing for offshore oxygenated water to be exchanged with nutrient-rich, but
 63 oxygen-depleted, nearshore water. Cross-shelf transport usually requires ageostrophic flow,

since geostrophically balanced flow will tend to follow topographic contours, often providing a barrier to lateral exchange (Brink, 2016). Mechanisms of cross-shelf exchange include internal waves and instabilities in shelf-break fronts. However, these mechanisms are often smaller in magnitude to intermittent three-dimensional exchange, driven by eddying, and often catalyzed by topographic irregularity (Barth et al., 2000).

Here we present detailed *in-situ* observations from the southern Vancouver Island shelf, collected in summer 2013, and sampled by a rapid profiling vehicle equipped with a CTD and oxygen sensor, supplemented by traditional hydrographic surveys bracketing the high resolution observations by a month. The shelf has complicated bathymetry (figure 1), with a simple shelf geometry poleward of our study site, but widening in the lee of La Perouse Bank, and incised by the Juan de Fuca canyon, equatorward. Water from the Strait of Juan de Fuca flows poleward as a buoyant current that hugs the coast (Thomson et al., 1989; Hickey et al., 1991), while shelf water flows equatorward in the summer under upwelling conditions, both forced by local winds and via tele-connections with the long, homogenous shelves equatorward off Washington and Oregon (Hickey et al., 1991; Thomson & Krassovski, 2015; Engida et al., 2016). Trapped between these two currents is a region of relatively homogenous water that has been termed the Juan de Fuca Eddy (Freeland & Denman, 1982; Freeland & McIntosh, 1989; Foreman et al., 2008; MacFadyen & Hickey, 2010), denoted “EDDY” below.

A goal of our study was to understand how the EDDY persists and how it exchanges water properties with offshore water. We focus on water deeper than 50m, below the summer mixed layer, because this water is trackable with water mass properties, whereas the EDDY is often studied from the point of view of the surface circulation [e.g.][macfadyen hickey10](#). Past studies have found low oxygen concentrations in the EDDY, and inferred that water is upwelled from the California Undercurrent from as deep as 400 m (Freeland & Denman, 1982; Dewey & Crawford, 1988). This inference was based on the assumption that oxygen is conservative, and hence water in the eddy had to come from the oxygen minimum zone found further offshore (Mackas et al., 1987). This lead to hypotheses that perhaps the EDDY was fed by waters being drawn up a spur canyon (called the Spur Canyon) via ageostrophic transport from offshore to onshore due to low pressure in the EDDY center (Weaver & Hsieh, 1987). Below, we will argue that there is no evidence of such transport and that oxygen is likely low because of local consumption due to respiration.

A second goal of our study was to better understand cross-shore exchange between shelf and offshore water. Cross-shore transport is supplied by Ekman layers in simple geometries under wind forcing. However, in many locations there is also evidence of filaments and wholesale separation of shelf currents into the deep ocean. Along the Vancouver Island shelf, large filaments or instabilities of the coastal current have been inferred using satellite images (Ikeda & Emery, 1984; Thomson & Gower, 1998). Direct observations of such filaments have been made further to the south off Cape Blanco (Barth et al., 2000), and off other coasts (Relvas & Barton, 2005). Net cross-shore transport of nutrients and chlorophyll have been found in hydrographic surveys off Vancouver Island (Mackas & Yelland, 1999), and associated with mesoscale features in geostrophic velocities and in satellite observations. The mechanisms driving such separations are poorly understood, but hypotheses include coastal hydraulics leading to along-shore trapping of coastal waves (Dale & Barth, 2001), wind stress curl variations (Castelao & Barth, 2007), induced relative vorticity due to stretching of parcels that overshoot their initial isobaths due to a sudden change in downstream bathymetry dasaro88, and the non-linear breaking of large-scale meanders due to baroclinic instability between the wind-driven current and the California Undercurrent (Ikeda et al., 1984; Batteen, 1997).

In this paper we present observations of water masses on the Southern Vancouver Island Shelf collected in 2013 (section 2), presenting the data in a number of ways to highlight the important processes, with a focus on the offshore side of the EDDY region (section 3) where we consider the age of the EDDY, the steadiness of the front separating the EDDY and the

117 offshore water, properties along the spur canyon that was believed to feed the EDDY, and
 118 a large offshore tongue of the shelf-break current and its intrusion into the interior. We
 119 discuss the origin of the EDDY and the implications of the separating jet (section 4).

120 **2 Site and Methods**

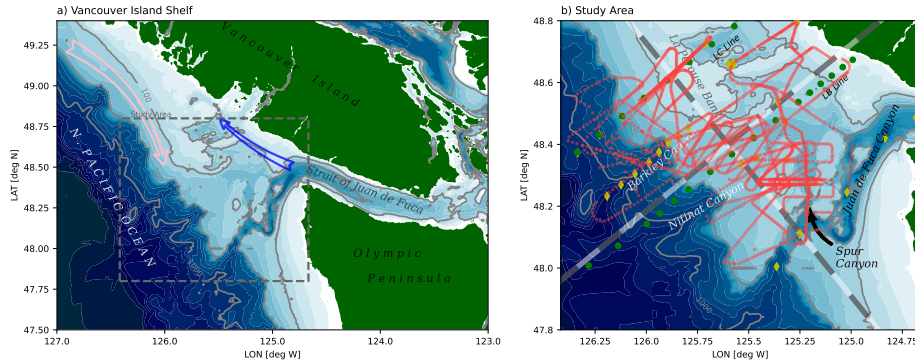


Figure 1. a) Study site on the Vancouver Island Shelf. The blue arrow indicates the direction of the Vancouver Island Coastal Current, and the pink arrow indicates southward flow of the coastal upwelling current. The dashed box indicates the approximate limits of the study area. b) The study area with hydrographic casts from the La Perouse cruises along the LB and LC Lines (green dots), hydrographic casts during the Falkor cruise (yellow diamonds), and finescale Moving Vessel Profiler casts (red dots). The coordinate system used for this paper is shown with alternating grey and white bands at 10-km intervals in the along- and cross-shore directions.

121 The study site was the southern portion of the Vancouver Island Shelf (figure 1a), a
 122 particularly complicated region due to the bathymetry and varied forcing. At the south end
 123 of the study site is the Juan de Fuca canyon, which feeds dense water into Juan de Fuca
 124 Strait. This dense water is mixed with fresh water from the Fraser River at the sills and
 125 archipelagos further inland and fluxes out the Strait again, where it turns poleward along
 126 Vancouver Island to form the Vancouver Island Coastal Current. The Juan de Fuca Canyon
 127 has a notable spur canyon (Spur Canyon), that incises the shelf towards the north into the
 128 study site (figure 1b). The rest of the shelf is punctuated by a series of banks and shallow
 129 basins. La Perouse bank separates the outer shelf from a deeper inner basin and forms the
 130 poleward boundary off where the shelf widens abruptly south of 48.5 N. Equatorward, the
 131 shelf widens further, and the shelf break has a series of submarine canyons, in particular
 132 Nitnat Canyon and Barkley Canyon.

133 We present observations from La Perouse hydrographic surveys along the LB and LC
 134 lines, collected aboard the *CCGS Tully* from 2013-05-30 to 2013-05-31 (“May”), and 2013-
 135 09-07 to 2013-09-09 (“September”). These lines span the 50 m isobath to deep offshore,
 136 with casts every 7.5 km across shelf. The data comes from a lowered Seabird 9-11 CTD,
 137 with an SBE 43 oxygen sensor. Oxygen data have been corrected against bottle casts, and
 138 the CTD corrected for sensor offsets and thermal lags.

139 Below, we focus on finescale surveys carried out from 2013-08-21 to 2013-08-30. Data
 140 were collected from the *R/V Falkor* with an ODIM Brooke-Ocean Moving Vessel Profiler
 141 (MVP). The MVP was equipped with an AML Oceanographic CTD, and a Rinko Oxygen
 142 sensor with a 7-s response time foil. The MVP profiled to depths of 200 m or to within 5 m
 143 of the seafloor, whichever was shallower, and dropped at a speed of approximately 3 m s^{-1} .
 144 Data collection took place while the ship cruised at speeds between 5 and 8 kts, usually at

145 around 6 kts, to enable fine horizontal spacing of the casts, with typical spacing of 800 m
 146 in deep water, and less in water shallower than 200 m. Data is reported for the downcast,
 147 which mostly follows a vertical path. The rapid speed of the profiling makes the oxygen
 148 measurements somewhat coarse, and probably biased due to the phase lag of the sensor, so
 149 we treat these qualitatively in this paper.

150 Unfortunately, neither vessel had an operational acoustic Doppler profiler during the
 151 cruises with which to make water velocity measurements.

152 Winds during the cruises were typical for the west coast of Vancouver Island, with
 153 upwelling favorable winds during July and early August (figure 2). During the finescale
 154 survey, and for the week previous, the winds were intermittently downwelling favorable.
 155 Note that this locale is strongly affected by coastally trapped waves from further south,
 156 so doming of near-bottom isopycnals often persists despite local wind forcing, and takes a
 157 finite amount of time to spin down (Thomson & Krassovski, 2015; Engida et al., 2016).

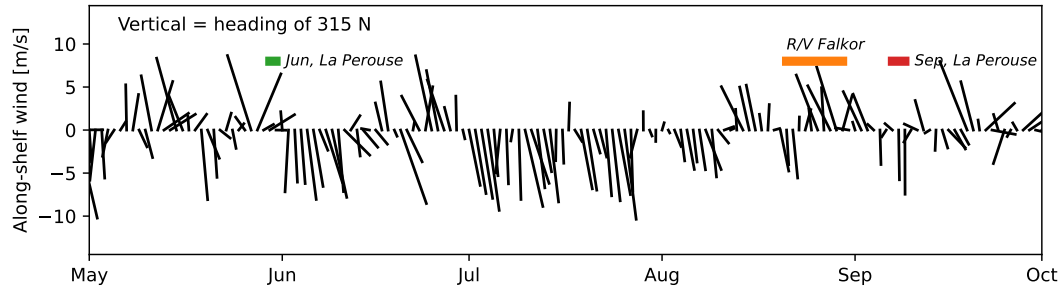


Figure 2. Wind from the La Perouse buoy (DFO, 2022). The vertical direction is along-shelf (chosen as a heading of 315 N), so vectors pointing straight down represent upwelling winds. The wind components have been low-pass filtered to one-day averages. The timing of the surveys discussed in the paper are shown as colored bands.

158 3 Observations

159 3.1 Early and late summer hydrographic surveys

160 Hydrographic sections along the LB and LC lines highlight summer conditions on the
 161 Southern Vancouver Island Shelf and indicate some of the features we are focusing on in
 162 this paper (Figure 3). During both surveys, and along both lines, there is clear evidence of
 163 upwelling, with the 26.4 kg m^{-3} isopycnal reaching from 130 m depth offshore to shallower
 164 than 85 m over the shelf. This upwelled water tends to be low in oxygen and cool. Further
 165 onshore, the Vancouver Island Coastal Current hugs the coast, where isopycnals tilt back
 166 down and water is warmer than offshore.

167 The Juan de Fuca Eddy region is observed along the LB Line (figure 3, bottom three
 168 rows), mostly inshore of 0 km. This water is cooler and lower in oxygen than along the same
 169 isopycnal further offshore. Near the surface, the isopycnals are domed, and the low-oxygen
 170 anomaly extends as high as the thin surface mixed layer.

171 The water upstream of the EDDY region, along the LC line, is less mixed than the
 172 EDDY water (figure 3, top three rows). It does not show as much drawdown of oxygen, and
 173 is warmer, at least offshore of La Perouse bank ($X \approx 5 \text{ km}$). Based on these properties,
 174 offshore water does not appear to make it over La Perouse bank into the basin onshore, or
 175 if it does, it does so intermittently. Note that the water along the 26.4 kg m^{-3} isopycnal

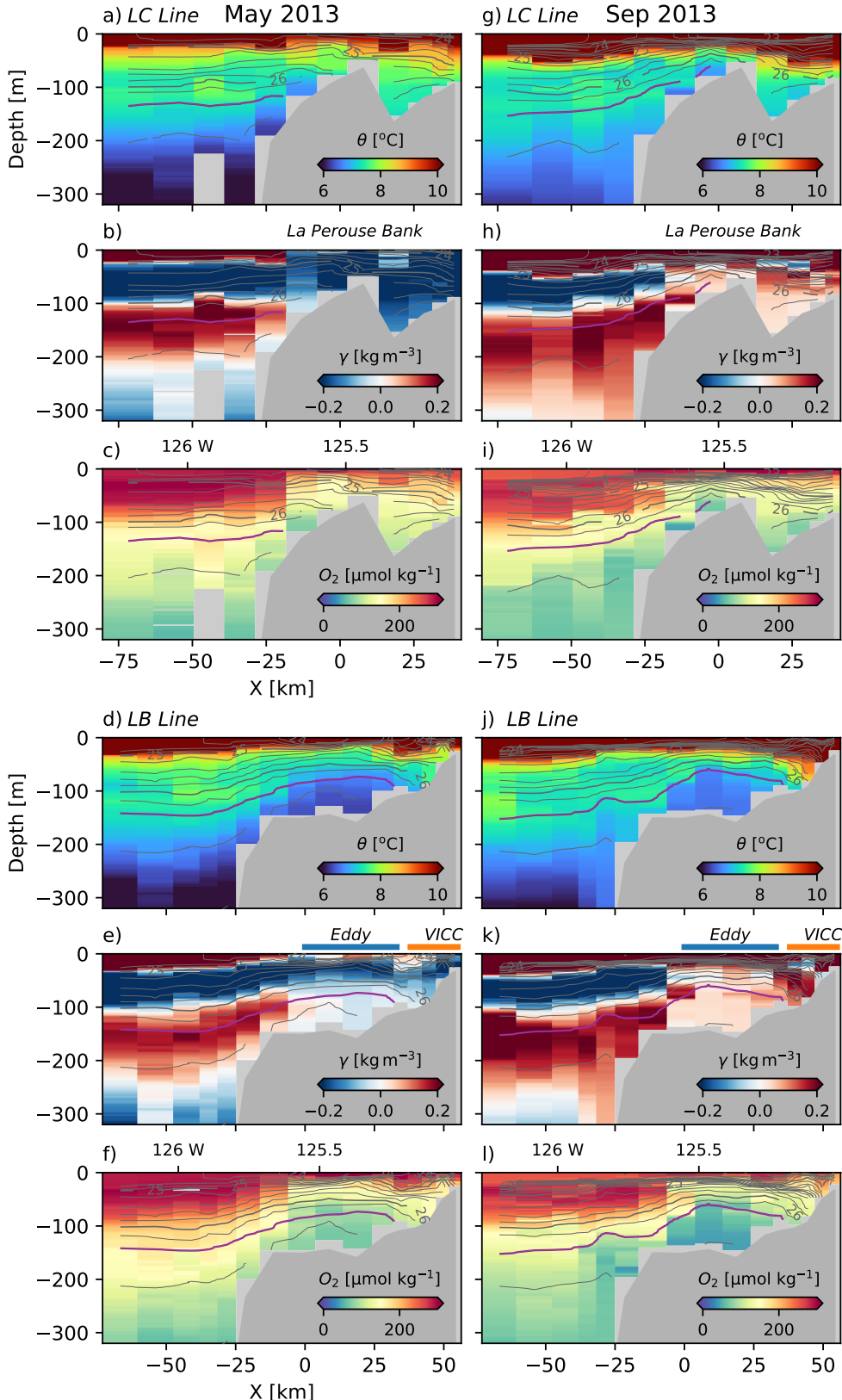


Figure 3. Observations along LC Line in May (a–c) and Sep (g–i) and LB lines in May (d–f) and Sep (j–l). X is across-shelf distance in the coordinate system shown in figure 1. Potential density is contoured every 0.2 kg m^{-3} , with the 26.4 kg m^{-3} colored magenta. Potential temperature, θ , spice anomaly, γ and oxygen concentration, O_2 , are colored for each section.

176 becomes cooler and lower in oxygen where it intersects the shelf, consistent with both
 177 enhanced mixing near the shelf and with drawdown of oxygen by respiration.

178 The contrast in onshore and offshore waters can be clearly traced in temperature-
 179 salinity (θ -S) anomalies along isopycnals (figure 4a). Denser than 26.6 kg m^{-3} , the deep
 180 water masses found offshore are largely homogenous. In the lighter water masses, there are
 181 distinct differences between warm and salty offshore water compared to water on the shelf
 182 at the same densities.

183 We use a spice anomaly defined as relative to a straight line in θ -S space (figure 4)
 184 representing an approximate mixing line for water in the EDDY, and passing through the
 185 points 7.75°C , 30 psu and 6.6°C , 35 psu. Spice anomaly for a given water sample at
 186 density σ_θ is given by $\gamma = \alpha(T - T_0(\sigma_\theta)) + \beta(S - S_0(\sigma_\theta))$ where $T_0(\sigma_\theta)$,
 187 where $S_0(\sigma_\theta)$ are the temperature and salinity along the mixing line at the same density as the water sample.
 188 The sign convention is that a positive anomaly is warmer and saltier than data along the
 189 mixing line.

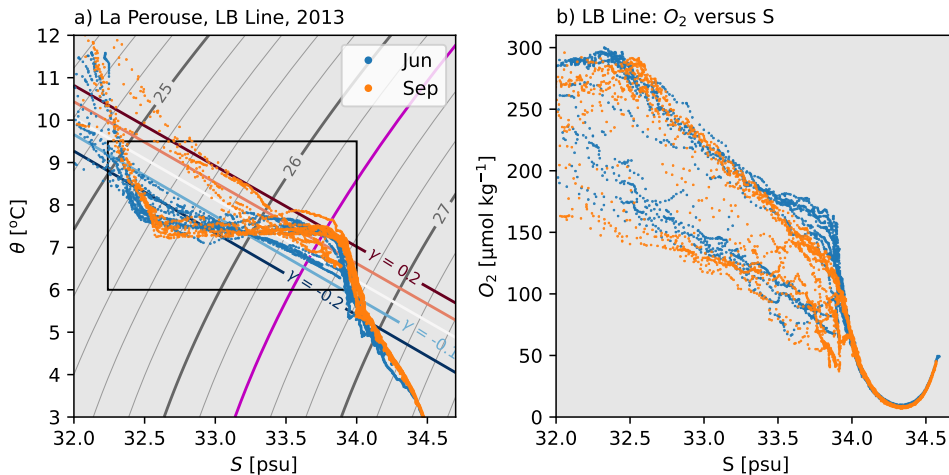


Figure 4. a) Potential temperature, θ , versus salinity, S , for the La Perouse data shown in figure 3; potential density is contoured every 0.2 kg m^{-3} , with the 26.4 kg m^{-3} colored magenta. A definition of spice anomaly is shown in this plot, and discussed in the text. The rectangle is the $\theta - S$ range used in figure 5 below. b) The same data with oxygen concentration versus salinity.

190 Using this metric of spice anomaly, offshore water tends to have high absolute values
 191 (figure 3, middle rows), with a positive-anomaly layer (red) centered at 26.4 kg m^{-3} sand-
 192 wiched between negative-anomaly layers above and below. On the shelf ($-10 \text{ km} < X <$
 193 30 km), the distinct $\theta - S$ masses are attenuated and much closer to the defined mixing line
 194 than the offshore water (closer to white in color in figure 3).

195 There are temporal changes over the summer. Away from the surface, water has
 196 upwelled from deeper depths by September, but the offshore water maintains the same water
 197 mass characteristics through the summer. Hugging the coast ($X > 30 \text{ km}$), the Vancouver
 198 Island Coastal Current warms during the summer, and the spice anomaly goes from negative
 199 to positive. In the EDDY, the water stays near the mixing line, but is cooler in the spring
 200 (figure 3, LB Line, left-hand column: slightly negative spice anomaly) and warms during
 201 the summer (figure 3, LB Line, right-hand column: slightly positive spice anomaly).

202 Oxygen concentration in both surveys has a similar dichotomy between the EDDY and
 203 offshelf water. Water found in the EDDY has oxygen concentrations $100 \mu\text{mol kg}^{-1}$ lower on

204 the shelf than offshelf (figure 3, figure 4b). The very deepest water ($S \approx 33.9$ psu) on the
 205 shelf shows a further $50 \mu\text{mol kg}^{-1}$ decrease in concentration between May and September
 206 along the LB line.

207 3.2 Finescale surveys

208 3.2.1 Overview

209 The finescale surveys covered most of the EDDY region, with an emphasis on the
 210 offshore edge near the shelfbreak front (figure 1). For water denser than 26 kg m^{-3} , there
 211 are three distinct water masses sampled on the shelf (figure 5). The first is the offshore
 212 water, which tends to be warmer, and hence has a positive spice anomaly ($\gamma \approx 0.2 \text{ kg m}^{-3}$
 213 along $\sigma_\theta = 26.4 \text{ kg m}^{-3}$). The second is water in the EDDY, which during this survey
 214 was found along the straight mixing line in $\theta - S$ space (figure 5, $\gamma \approx 0 \text{ kg m}^{-3}$ along
 215 $\sigma_\theta = 26.4 \text{ kg m}^{-3}$). Between these two water masses, there is a less populous mass (figure 5,
 216 $\gamma \approx 0.1 \text{ kg m}^{-3}$ along $\sigma_\theta = 26.4 \text{ kg m}^{-3}$) that we demonstrate below is found on the shelf
 217 poleward of the EDDY.

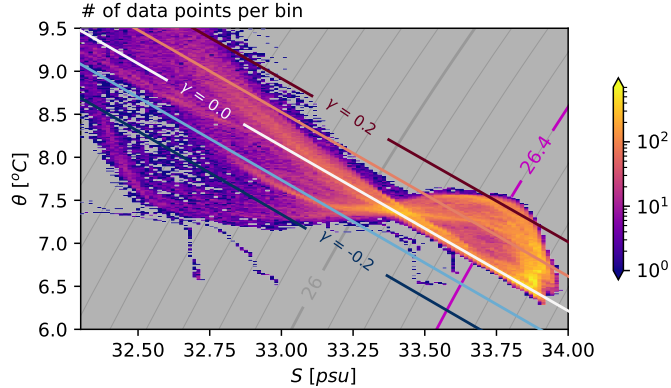


Figure 5. Binned sample density of salinity and potential temperature from the cruise, with a logarithmic color scale. Grey contours are potential density relative to the surface at intervals of 0.1 kg m^{-3} ; the magenta contour is the 26.4 kg m^{-3} isopycnal. Colored contours are spice anomaly, γ , relative to the white line labeled $\gamma = 0.0$.

218 In synthetic cross sections of spice anomaly, the EDDY is clearly identifiable as having
 219 low spice anomaly ($\gamma \approx 0 \text{ kg m}^{-3}$, figure 6c, d). This signature of well-mixed water extends
 220 from the seafloor to approximately 30 m depth, onshore of $X \approx 0 \text{ km}$. Despite lying along
 221 a mixing line, the EDDY water is still stratified. The high-spice water ($\gamma \approx 0.2 \text{ kg m}^{-3}$)
 222 is found offshore of the EDDY water, on the other side of a sharp $\theta - S$ compensated
 223 front. This front is even sharper in individual sections than in these composite sections (see
 224 section 3.2.3).

225 In contrast, the third population of partially mixed water between the EDDY and
 226 offshelf water (figure 5) is all found poleward of the EDDY region (figure 6a, b) as water
 227 with a weaker spice anomaly ($\gamma \approx 0.1 \text{ kg m}^{-3}$, pink colors). This water is generally found
 228 near the intersection of the upwelling water and La Perouse Bank, and is not as warm as
 229 offshelf water, indicating some mixing with offshelf water has taken place. Of note is that
 230 this intermediate water mass appears completely absent in the sections further equatorward
 231 (figure 6c, d), indicating that it is either mixed away or that it is advected elsewhere; we
 232 argue below that it is advected offshore in a large-scale tongue.

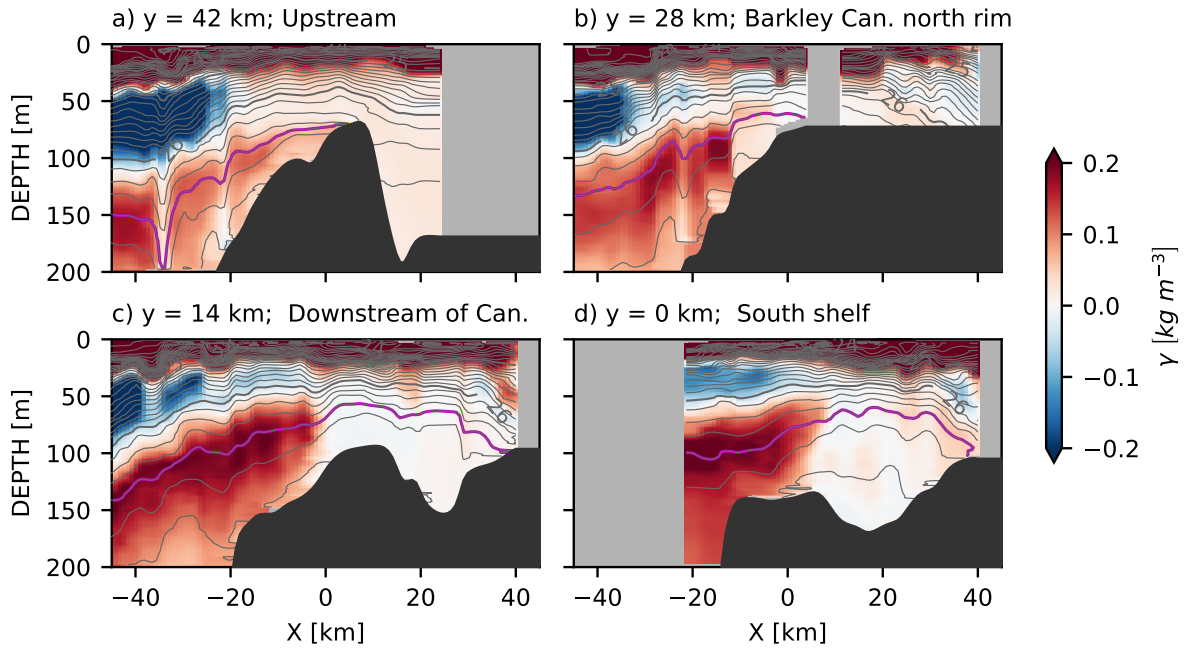


Figure 6. Synthetic sections of spice anomaly from the MVP data, projected along four lines from poleward (upstream of coastal current) a) to equatorward (downstream); the lines are shown in figure 1b). Isopycnals are contoured every $\sigma_\theta = 0.2 \text{ kg m}^{-3}$, with the $\sigma_\theta = 26.4 \text{ kg m}^{-3}$ isopycnal highlighted in magenta. Colors are spice anomaly as defined in figure 5. "BC" in panel (c) refers to Barkley Canyon.

Oxygen saturation sections show similar trends, with the low-spice anomaly water also having low oxygen saturation, while the strong negative spice anomaly shallower than $\sigma_\theta = 26.4 \text{ kg m}^{-3}$ has very high oxygen saturation; deeper water is also more oxygenated. Of note is that compared with the coarser sampling along the LC Line (figure 3), we see that the abrupt transition between offshore and EDDY water is also present in dissolved oxygen.

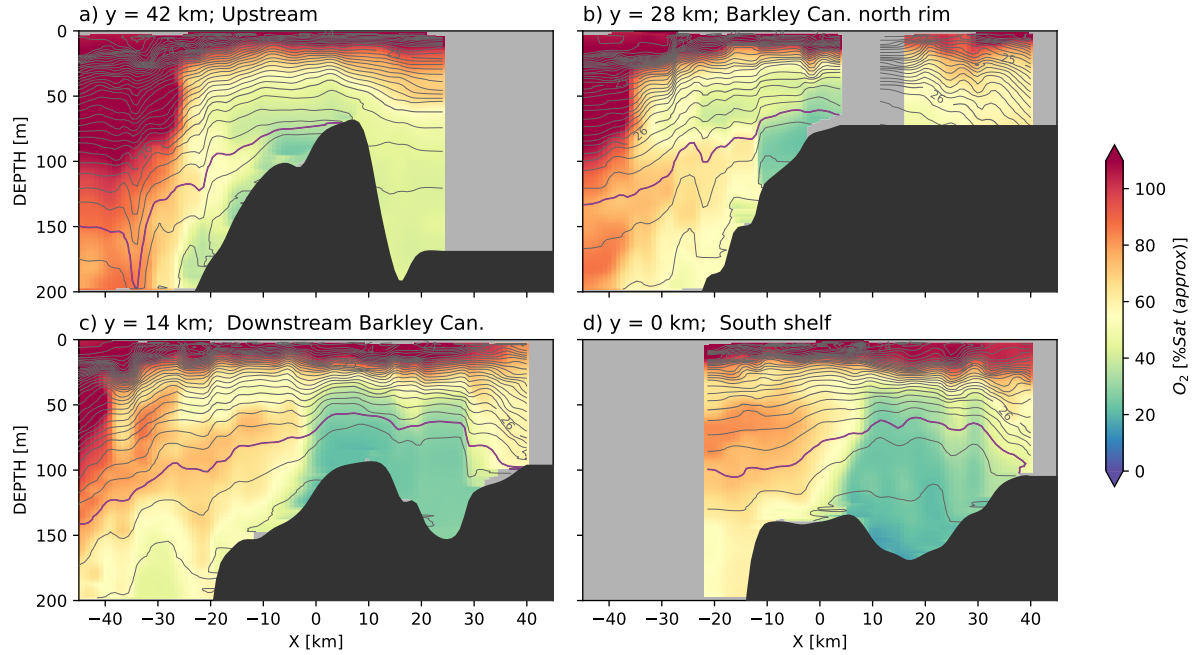


Figure 7. As in figure 6, for oxygen approximate saturation.

The spatial patterns are very clear when considering a map view of properties along the $\sigma_\theta = 26.4 \text{ kg m}^{-3}$ isopycnal (figure 8). There is a region onshore of the south tip of La Perouse Bank (approximately $44.5^\circ\text{N}, 125.75^\circ\text{W}$), that consists of water that is found along the mixing line (spice anomaly $\gamma \approx 0 \text{ kg m}^{-3}$) with low oxygen saturation. Offshore of this region is water that is very warm and salty in comparison ($\gamma > 0.15 \text{ kg m}^{-3}$), and relatively high in oxygen (saturations of approximately 60%). The region between these two water masses is very abrupt, and stretches from La Perouse Bank to a shallow bank just above the Juan de Fuca canyon (48.3°N and 125.4°W).

Poleward of La Perouse bank and Barkley Canyon, the water along the shelf has the weaker spice anomaly characteristic of the third water mass ($\gamma \approx 0.1 \text{ kg m}^{-3}$, light pink colors). This water is also somewhat lower in oxygen than water from offshore, though not as depleted as the water in the EDDY. This water appears to be pushed offshore just upstream of Barkley Canyon and replaced on the shelf by the warmer (high spice) offshore water.

3.2.2 Spur Canyon

The Spur Canyon leading from the Strait of Juan de Fuca has been implicated in allowing dense water to be upwelled into the EDDY. The sea surface is low in the middle of the EDDY, so it has been hypothesized that water moves up the Spur Canyon due to ageostrophic motion (Weaver & Hsieh, 1987; Freeland & Denman, 1982). This is difficult to infer from the observations collected here. Three transects up the canyon indicate that deep isopycnals slope up into the canyon (figure 9, to approximately 30 km). Continuing

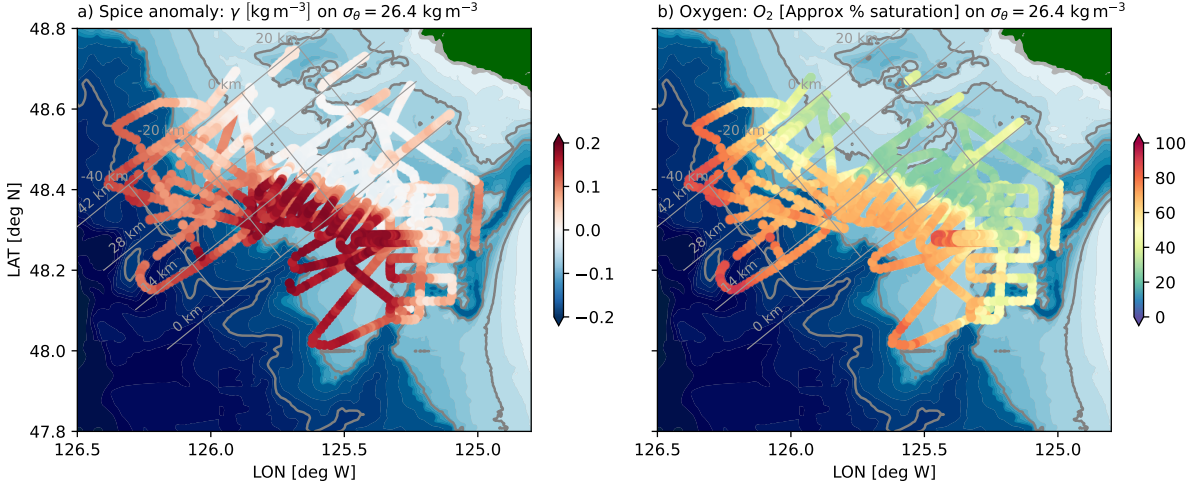


Figure 8. Spatial overview of a) the spice anomaly, and b) oxygen saturation on the $\sigma_\theta = 26.4$ kg m⁻³ isopycnal. Grey cross-slope lines are cross sections indicated in figure 6. Along-slope grey lines are every 20 km in the cross-slope direction, with $X = 0$ km near the 100-m isobath at the north end of the observation area.

across the EDDY, isopycnals are largely flat until they intersect the Vancouver Island Coastal Current (80 km). The deeper isopycnals are not found in the deeper basin northeast of La Perouse bank (70 km), thus the bank is a natural northern boundary of the EDDY.

Spice anomaly along the canyon indicates a transition from offshore water to EDDY water. Oxygen saturation behaves in a similar manner, though some of the incoming water has slightly lower oxygen than water inside the EDDY (not shown). Based on these sections, it is difficult to infer water motion up the canyon.

Much of the modified water in the Spur Canyon appears to come from the shelf to the west, but heavily modified by tidal mixing. A repeated tidal survey over the bank on the west side of the canyon shows a strong hydraulic response during onshore flow (17:58–21:00, figure 10). Dense water passes from the offshore side into the canyon, and plunges down the side wall before rebounding downstream. Note that the tide here is largely diurnal, so this onslope flow only occurs once a day. Given the stratification of $N \approx 6 \times 10^{-3}$ rad s⁻¹ and an overturning scale of 50 m, we might expect dissipation rates reaching $\epsilon \sim L^2 N^3 \approx 5 \times 10^{-4}$ m² s⁻³, which is more than three orders of magnitude higher than dissipation observed west of this location by Dewey and Crawford (1988). This estimate of turbulence dissipation rate implies a diapycnal diffusivity of $\kappa = \gamma\epsilon/N^2 \approx 1$ m² s⁻¹, assuming a mixing efficiency of $\gamma = 0.2$. Water spills over from the offshore front into the canyon during the onshore tide. This water is rapidly mixed with surrounding water such that its strong offshore spice values are attenuated.

The turbulence found on the canyon rim makes it ambiguous if there is water moving up the canyon or not. There is a general tendency along the canyon for higher spice water to be found offshore (figure 9) but it seems likely the source of the higher spice water is from over the bank rather than water being advected up the canyon. This tidally driven flow over the bank is the most significant source of high-spice offshore water into the eddy region identified during our surveys.

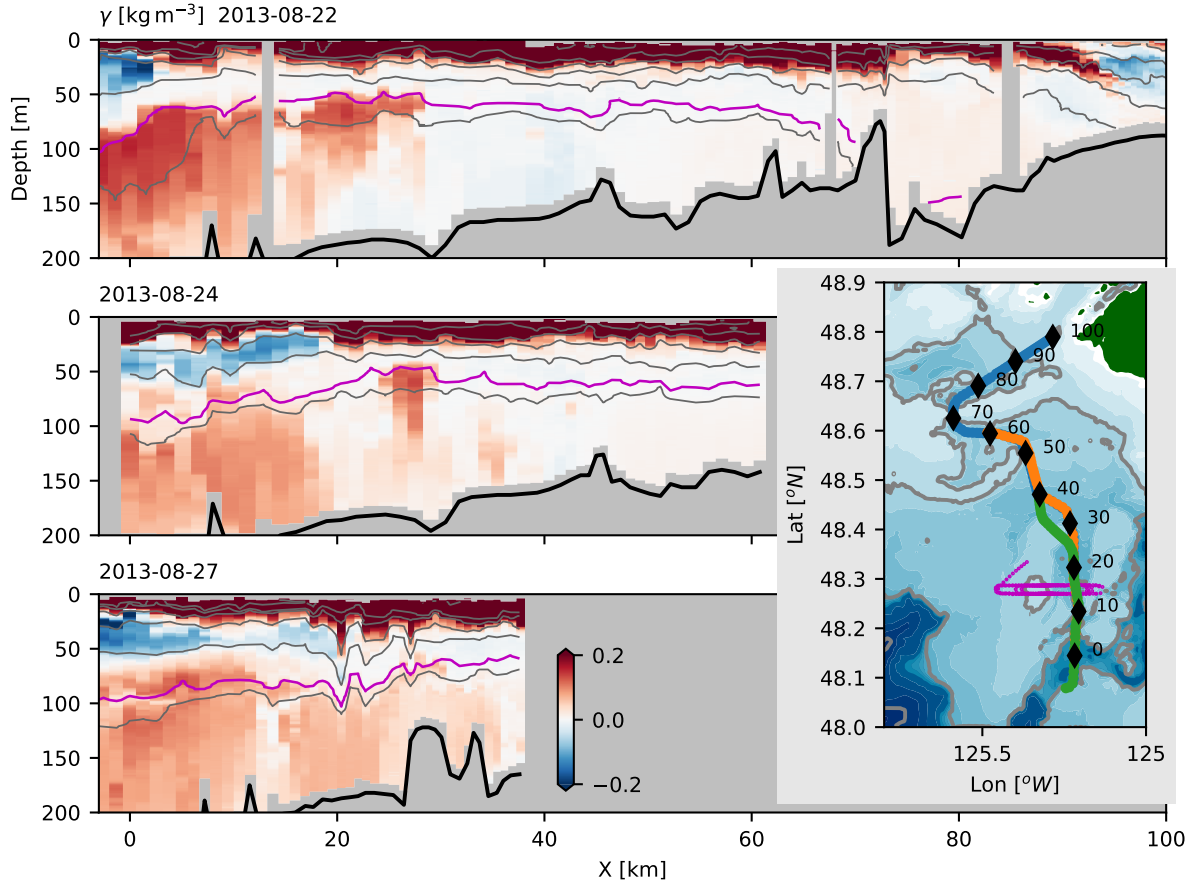


Figure 9. Spice anomaly surveys up the Spur Canyon, where X is along-canyon as defined in the map. Grey isopycnals are contoured every 0.5 kg m^{-3} , and the 26.4 kg m^{-3} isopycnal is shown in magenta. The seafloor is indicated with the thick black line. Map (lower right) shows the path taken during each survey in chronological order (blue, orange, and green). Magenta line is path taken during a cross-canyon survey (figure 10).

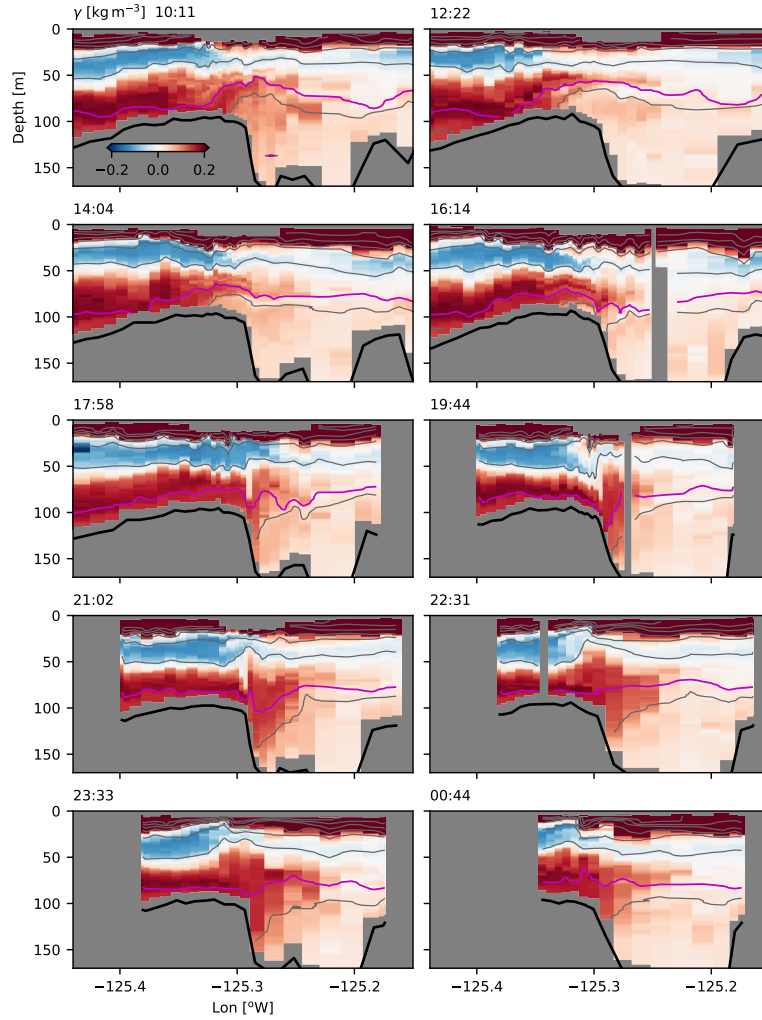


Figure 10. Spice anomaly observed in repeated, tide-resolving survey across the Spur Canyon, time is indicated in the upper left of each plot (29 August, 2013). Location of survey shown in figure 9 as a magenta line.

285 ***3.2.3 Frontal survey***

286 A systematic survey through the front between the offshore water and the EDDY water
 287 demonstrates the sharpness and persistence of this front (figure 11), suggesting that it has
 288 limited exchange with the offshore region.

289 The survey started close to shore, and passed through the Vancouver Island Coastal
 290 Current (along-track 0-10 km). The coastal current forms a buoyant front, and is fresher
 291 and colder than water at the same density. This front is relatively thick, greater than 20
 292 km wide, and has partially mixed water from the surface to the foot of the front ($\gamma \approx 0.1$).

293 Offshore of this coastal current, measurements were collected crossing the front be-
 294 tween the offshore water and the EDDY water 10 times, showing its evolution following the
 295 along-shore equatorward flow. First, as noted in the composite sections, isopycnals slope up
 296 from offshore onto the shelf. In the first crossing, the front is very sharp, (along-track dis-
 297 tance 50 km) though two small tendrils can be seen separating from the front on the inshore
 298 side. Similar tendrils are found on the second crossing, perhaps a bit more separated from
 299 the front (≈ 80 km), and on the third crossing (≈ 95 km). These tendrils are made of up
 300 partially mixed water. The subsequent passes have more of this partially mixed water, such
 301 that the partially mixed front is up to 5-km wide by the fifth pass (≈ 150 km). However,
 302 the deeper isopycnals retain a sharp front, and indeed the front appears sharp again by the
 303 seventh pass at all depths (≈ 200 km).

304 There is evidence of some warmer water swirling into Eddy, particularly along isopy-
 305 cnals deeper than 26.4 kg m^{-3} . Regions of warmer (and more oxygenated) water are found
 306 in tendrils at these depths (e.g. ≈ 170 km and ≈ 185 km). The overall effect is similar to
 307 what was seen in the Gulf Stream with similar observations (Klymak et al., 2016); there
 308 are two quite distinct water masses, the Eddy water and the offshore water, as seen in the
 309 $\theta-S$ plot (figure 11c) with only a small population of samples between these two. This
 310 distribution of $\theta-S$ properties is indicative of substantial isopycnal and vertical mixing, but
 311 even these populations are relatively cut off from the main water masses, indicating that
 312 they are well-mixed on their own, in short episodic events. Regardless, this front is very
 313 sharp given that it has no density signature, indicating that there is not strong advection
 314 from offshore into the EDDY region.

315 ***3.3 Separation of coastal water***

316 Upstream of the the sharp front between the low-spice EDDY and the high-spice off-
 317 shore water is a substantial mass of intermediate-spice water along the shelf (compare figure
 318 6a and c). If in geostrophic balance, this intermediate spice water is moving equa-
 319 torward along the shelf upstream of the EDDY, but is pushed offshore just upstream of
 320 Barkley Canyon (figure 12). There is a tongue of intermediate-spice water (γ is pink along
 321 26.4 kg m^{-3}) that separates from the shelf just west of 126°W . The surveys do not cross the
 322 full extent of the tongue, but it is at least 30 km wide. It also appears to end at approxi-
 323 mately 48.2°N . This intermediate-spice water reaches from relatively shallow isopycnals to
 324 at least 26.6 kg m^{-3} (figure 12, left panel). Unfortunately, we cannot track the fate of this
 325 water mass because isopycnals tilt down offshore, below the depth limit of the MVP. The
 326 25.5 kg m^{-3} isopycnal appears to have the tongue closer to the shelf than at 26.4 kg m^{-3} ,
 327 indicating strong three-dimensionality to this feature.

328 This separating tongue is embedded in the larger scale isopycnal tilt caused by the
 329 upwelling (figure 12, right panels), so it is difficult to see dynamically what is driving this
 330 offshore push. One possibility is that it is simple flow separation caused by the water not
 331 being able to make the sharp turn around La Perouse Bank. Whatever causes it, downstream
 332 of the separation, the water is replaced by offshore water with much higher spice values.

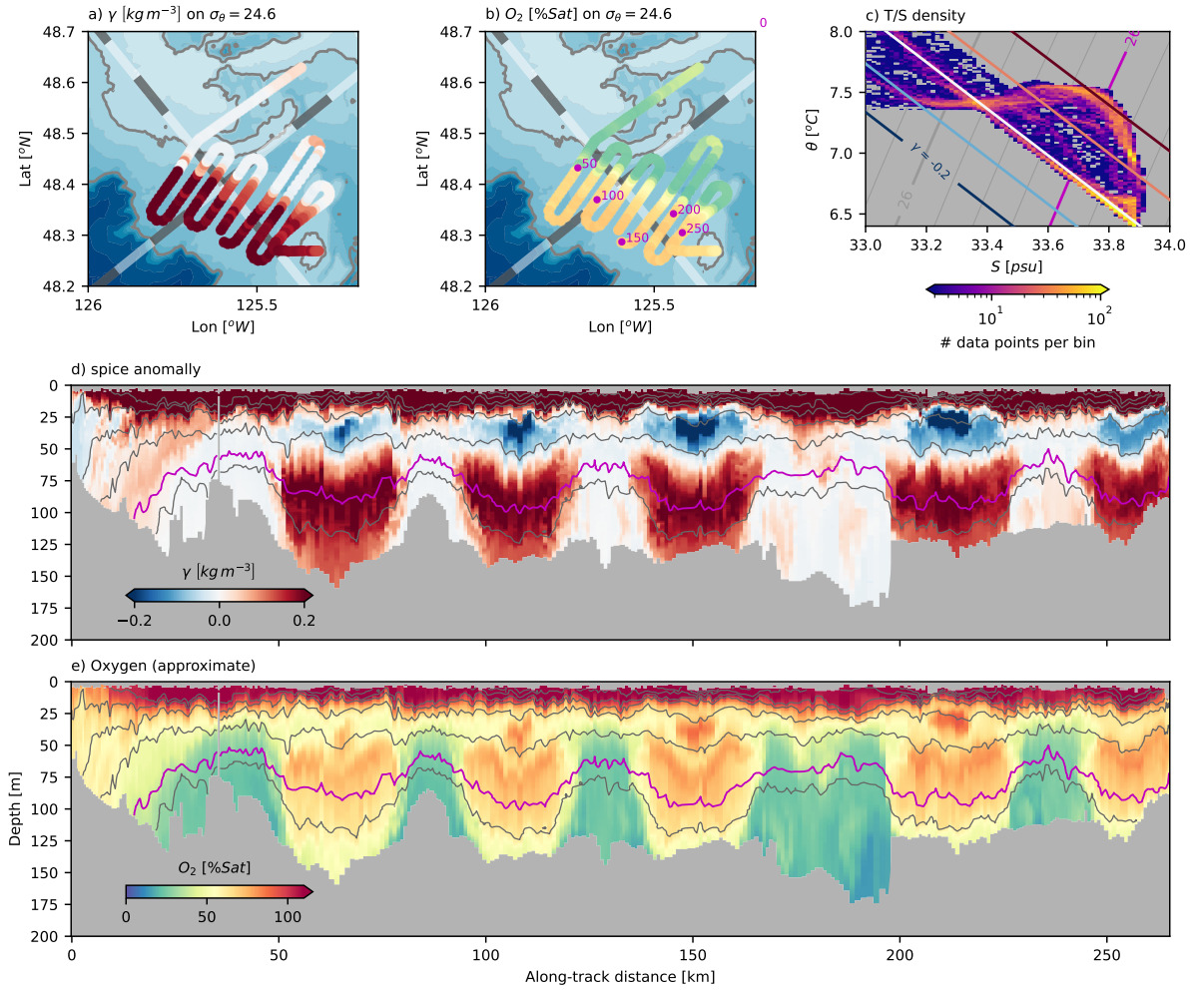


Figure 11. Data from the frontal survey a) spice anomaly along 26.4 kg m^{-3} . Grey-white alternating lines are the coordinate system, with 10-km alternating shades. b) oxygen saturation along 26.4 kg m^{-3} ; magenta dots correspond to distance along-track. c) density of data points (logscale) in this section of data. d) cross-section of spice anomaly along track. Grey isopycnals are contoured every 0.5 kg m^{-3} , and the 26.4 kg m^{-3} isopycnal is shown in magenta. e) cross-section of oxygen saturation.

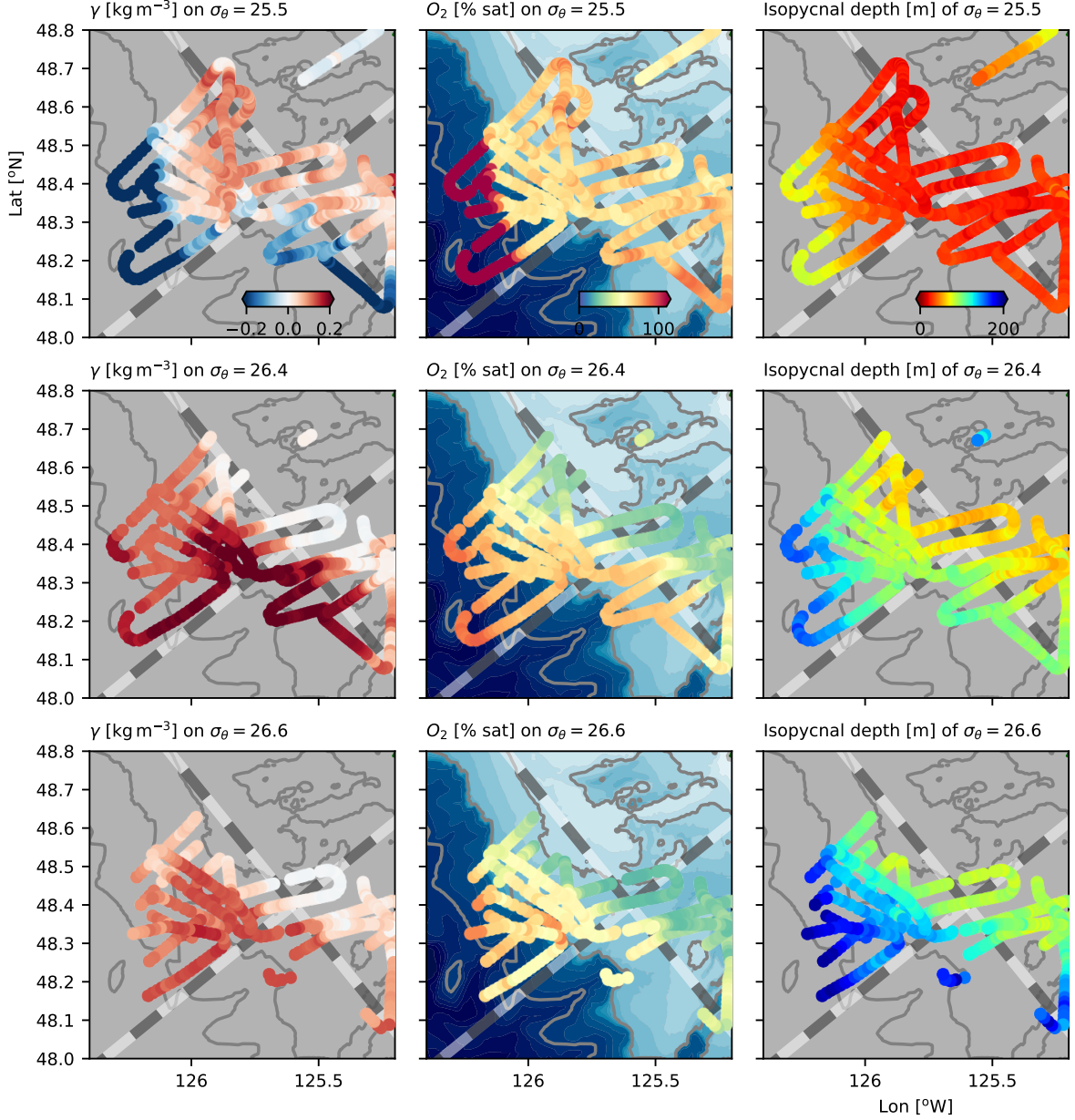


Figure 12. Isopycnal slices through showing the vertical structure of the water separating from the shelf, with the first row along 25.5 kg m^{-3} , second along 26.4 kg m^{-3} , and the third at 26.6 kg m^{-3} . First column is the spice anomaly, second is oxygen saturation, and the last column is depth of each isopycnal.

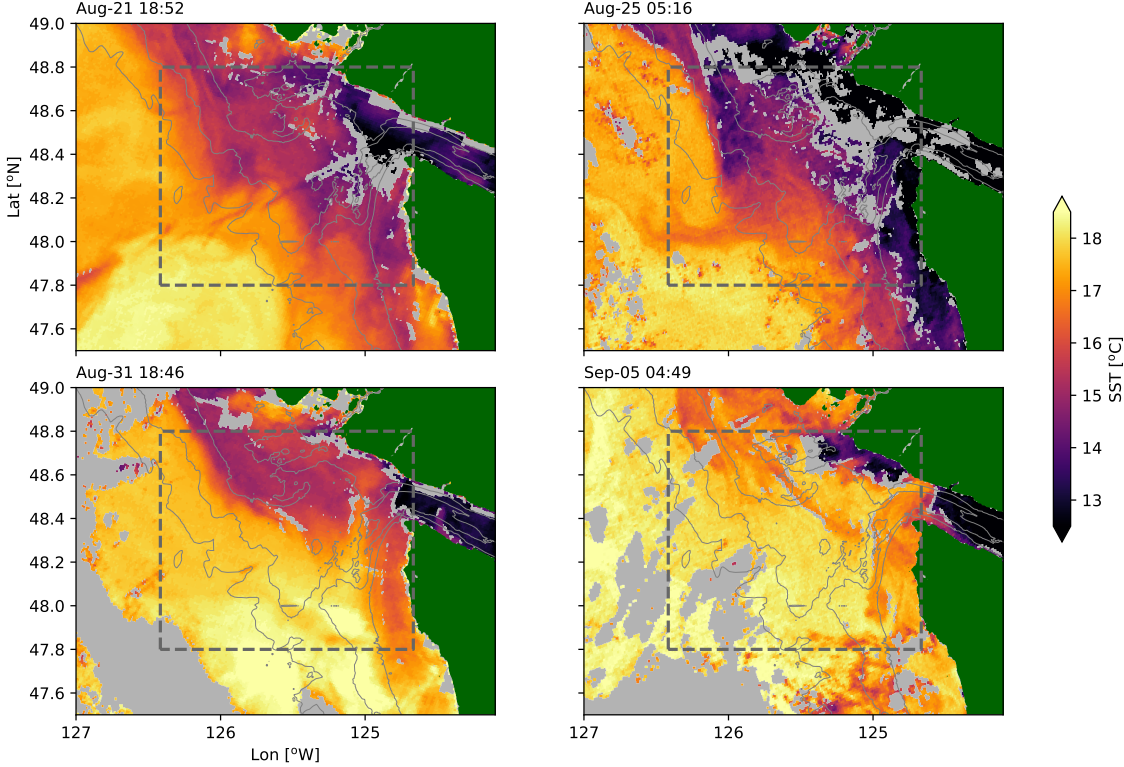


Figure 13. Sea surface temperature snapshots from the observation period. Grey areas are clouds; dashed gray line is the study area. Depths are contoured in thin gray lines at 200, 150 and 100 m. (OSI SAF, 2015)

There is a clear surface expression of the separating tongue in satellite imagery (figure 13). Water flowing equatorward along the shelf tends to be cooler than offshore water, likely due to mixing with the colder coming out of the Strait of Juan de Fuca. On August 25, there is a cold tongue of water separating from La Perouse bank, crossing isobaths and pointing south at 125.8°W . There is a cooler tendril streaming west at 48°N off the south end of this tongue. This feature is not as well-developed in the previous image (21 August) perhaps indicating that it is an evolving feature. By 31 August, there is no surface expression of the feature, though small tendrils of cooler water can be seen separating from La Perouse Bank. By 5 September, the water has significantly warmed, and the offshore anomaly does not appear to have a surface signature.

Satellite-based surface chlorophyll estimates show the same feature (figure 14) demonstrating the advection of high chlorophyll to the west side of the EDDY. They also show a relatively high-chlorophyll tendril to the west, again exiting the study region at approximately 48°N . The feature is relatively long-lived, on the order of one month. Inspection of images before August 5 were too obscured by clouds or did not show this feature. By September 6, we see the feature fading from the satellite image. Note that this feature is centered 0.2 degrees of latitude south of tongue that we observe deeper in the water column, again indicating that there is depth-dependent structure in the feature.

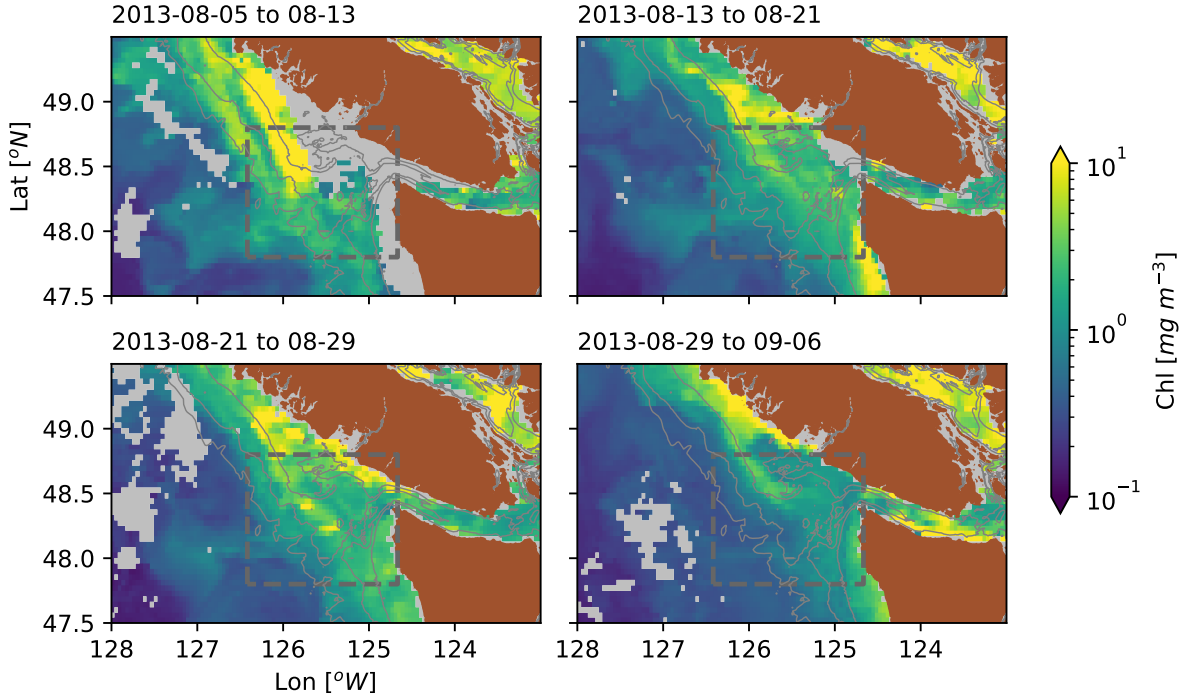


Figure 14. Surface chlorophyll density estimated from ocean color (Hu et al., 2012; NASA Ocean Biology Processing Group, 2017) over 8-day windows in 4-km bins. Gray regions had too many clouds to compute averages.

4 Summary and Discussion

The intensive sampling discussed here has demonstrated a few important features of the South Vancouver Island Shelf. The Juan de Fuca Eddy water is readily identified as falling along a mixing line in $\theta - S$ space, compared with offshore water that was warmer and saltier (high-spice anomaly). There was not strong evidence of the EDDY being supplied by water moving up the Spur Canyon during our observations, but the Spur Canyon was a site of hydraulic cross-canyon flows in which we infer significant mixing. There is a sharp and persistent temperature-salinity compensated front between offshore water and the partially mixed EDDY water. Finally, upstream of the EDDY, water in the equatorward shelf current has intermediate spice anomaly, and is seen to separate from the shelf at the point of an abrupt bend in an underwater bank. The water mass crosses isobaths and is ejected into the interior. This separation event can also be observed from satellite measurements of seafloor temperature and chlorophyll. Thus the water that is offshore of the EDDY appears to have been brought onto the shelf in exchange for the offshore ejection of shelf water via this tongue.

4.1 Age and source of the EDDY water

The source of water and formation mechanism of the Juan de Fuca Eddy has received substantial attention, however, the observations of EDDY waters being found along a tight mixing line in $\theta - S$ space has not previously been noted. The deepest water in the EDDY could originate along the $\theta - S$ line from approximately 5.5°C to 7.5°C (figure 4a), which in the open ocean spans depths from 420 m to 70 m. Mackas et al. (1987) attempted to determine the origin of the water by including oxygen as a third variable to resolve the

373 ambiguous θ - S relation. However, as figure 4b makes clear, oxygen does not appear to be
 374 a conserved property in the EDDY, with concentrations up to $150 \mu\text{mol kg}^{-1}$ lower in the
 375 EDDY than the water found offshore, and in a way that definitely cannot be the result of
 376 conservative mixing. As a best guess, if the water in the deepest part of the EDDY came
 377 from a vertical mixture of the water at 26.5 kg m^{-3} and an equal distance down in density
 378 space of 26.7 kg m^{-3} , then the deepest water in the EDDY may be coming from a depth of
 379 250 m. This is a typical upwelling depth for coastal flows, and may not require extra input
 380 up the Spur Canyon as posited by Freeland and Denman (1982).

381 We found little evidence of flow up the Spur Canyon or, if there is, then the mixing in
 382 the canyon is intense enough to remove the θ - S signature of offshore water within 20 km of
 383 the canyon mouth (figure 9). We did find substantial evidence of mixing in the canyon, but
 384 the primary pathway of high-salinity water into the canyon appears to be due to tidal flow
 385 over the banks on the west side (figure 10), rather than flow up the canyon. However, it is
 386 worthy of note that upwelling winds had ceased at the point of these observations (figure 2),
 387 so the offshore surface pressure gradient may be reduced, leading to reduced ageostrophic
 388 upwelling in the canyon. Whether the cessation of winds would also lead to a reduction of
 389 the low sea level height in the center of the EDDY that may drive up-canyon flow is an open
 390 question.

391 There is evidence of aging of the water in the EDDY between late spring and late
 392 summer (figure 3), with a reduction of oxygen in the EDDY over this time span. If we
 393 posited that the reduction was all in the same water, then the oxygen consumption rate
 394 over the time between the late-May and early September cruises would be on the order of
 395 $0.5 \mu\text{mol kg}^{-1}\text{d}^{-1}$. This is on the low side of estimates of apparent oxygen utilization rates
 396 in continental upwelling systems, which are between 1 and $5 \mu\text{mol kg}^{-1}\text{d}^{-1}$ (Dortch et al.,
 397 1994). So it seems possible the EDDY had enough exchange with the surrounding water for
 398 the residence time to have been less than the full time period from late May to September.
 399 Note that during the May cruise, the water in the EDDY is slightly cooler than the mixing
 400 line, and during the September cruise is slightly warmer than the mixing line, so the water
 401 in the EDDY is evolving seasonally, and probably affected by the water temperature in the
 402 Vancouver Island Coastal Current and the amount of water getting through the onshore
 403 front.

404 The water is mixed enough in the EDDY that it falls along a mixing line, though it
 405 remains vertically stratified. The amount of homogenization is such that either the mixing
 406 is very strong, or the water is retained in the EDDY for a long time. The amount of
 407 turbulence required to homogenize 100 m of water over 90 days is $\kappa \approx 10^{-3} \text{ m}^2\text{s}^{-1}$. Given
 408 that the diffusivity implied in the cross-channel surveys was (very) locally on the order of
 409 $\kappa_\rho = 10 \text{ m}^2\text{s}^{-1}$, this number is not outrageous if we think that such high dissipation is
 410 found in 10^{-4} of the water column. We can more carefully quantify this by considering
 411 a synthetic profile of temperature and salinity based on an offshore profile, extrapolated
 412 from the bottom of the 200-m cast to 250 m, assuming that the temperature and salinity
 413 at 250 m are $6.2 [\text{°C}]$ and 34 psu respectively (figure 15). Water at the offshore station
 414 was warmer than onshore, so the profile was also linearly interpolated to a surface value
 415 of $(12 \text{ °C}, 31.6 \text{ psu})$. The profile was then linearly compressed into a depth range of 150
 416 m representative of the shelf depth in the dense pool, and subjected to mixing with a
 417 constant diffusivity of $\kappa = 10^{-3} \text{ m}^2\text{s}^{-1}$, with the surface and bottom values pinned under
 418 the assumption that the near-bottom source and surface waters are replenished from a large
 419 reservoir. Similar to the naive scaling, the T-S relationship does not approach a straight
 420 line until after approximately 60-100 days, or until the mixing affects a vertical length scale
 421 of $\lambda = (\tau\kappa)^{1/2}$ that is greater than $\approx 70 \text{ m}$.

422 The sharpness of the front with the EDDY and the offshore water is intriguing. It was
 423 persistent for the duration of our detailed survey (figure 8), and, so far as we can tell with
 424 the limited resolution of the hydrographic surveys, was present during the bracketing La

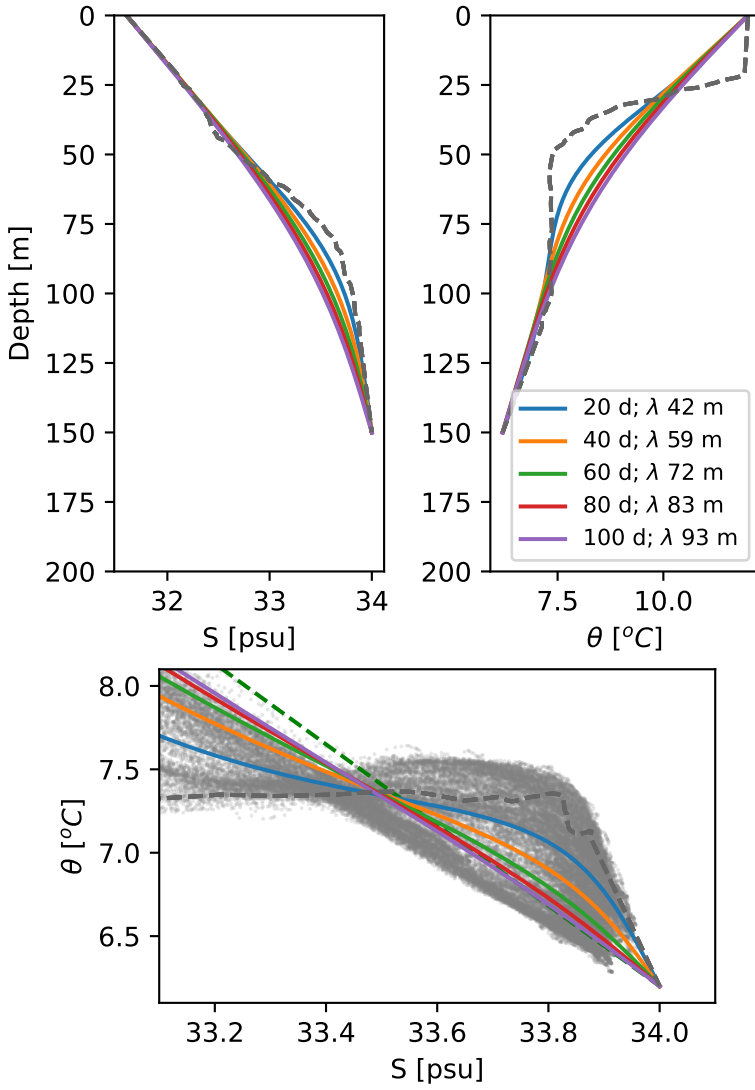


Figure 15. Mixing model assuming constant eddy diffusivity of $\kappa = 10^{-3} \text{ m}^2 \text{s}^{-1}$ acting on an offshore temperature and salinity profiles compressed from 250 thick to 150 m thick (grey dashed lines). Profiles are pinned to the deep $\theta - S$ value at (34 psu, 6.2 °C), and a shallow one at (31.6 psu, 12 °C). The green dashed line is the mixing line defined in the text.

425 Perouse cruises. There is not any substantial bathymetry blocking the onshore incursion of
 426 water at this location, so there must be a dynamic barrier.

427 Numerical simulations of this region reported by (Sahu et al., 2022) using a NEMO
 428 36th-degree regional model indicate that there is more rapid exchange between the deep
 429 EDDY water and the rest of the coastal ocean. In this model, the region where the EDDY
 430 resides has velocities equal or greater than other parts of the shelf, and water has an ap-
 431 proximate residence time of less than 20 days. The EDDY water in the model does develop
 432 a distinct θ - S signature, but not along a sharp mixing line as observed. It also has a front
 433 with the offshore water, but the front is substantially wider than that observed here.

434 Overall, it would be an improvement to our understanding of the EDDY if we could
 435 sample the shelf more persistently. The EDDY was already well-formed by the May La
 436 Perouse cruise, and seems to evolve slowly during that time. Capturing its formation,
 437 presumably earlier in the spring, as well as its evolution through the year, would be valuable
 438 in understanding retention and exchange on this productive part of the shelf.

439 4.2 Offshore exchange of shelf water

440 The (apparent) displacement of shelf water from La Perouse Bank is a dramatic de-
 441 parture from geostrophically balanced isobath-following flow. Eddies have been known to
 442 separate from irregular coastal topography, both at the surface (Barth et al., 2000) and
 443 deeper in the water column (Pelland et al., 2013). It has been recognized that instabilities
 444 lead to exchange between the open ocean and the shelf at this location (Ikeda & Emery,
 445 1984, 1984). However, observations of the wholesale replacement of shelf water by a new
 446 water mass from offshore are rare. In these observations it is clear that water from as deep
 447 as 150 m is separating from the shelf and moving offshore (figure 8, figure 12).

448 Satellite imagery makes it clear that there is often exchange between coastal and deep
 449 waters along the Vancouver Island shelf (figure 16). Most years there are three of four
 450 large filaments from the shelf into the open ocean, many of them over 100 km long. This
 451 length scale is longer than the 60 km inferred for this region by Ikeda et al. (1984) using a
 452 four-layer instability analysis. It is possible that there is spatial locking of these features,
 453 with a persistent separation at the north tip of Vancouver Island, and a strong tendency
 454 for one at 49.5 N. There is also evidence of separation events in most of the years,
 455 with 2011 being the only clear exception. General baroclinic instability of the upwelling
 456 front is a possible mechanism to drive offshore exchange (Ikeda et al., 1984; Durski & Allen,
 457 2005), but this tends to be shallow, with smaller-scale instabilities that will not extend as
 458 far into the interior ocean as observed here. Rather it seems likely that the topographic
 459 change engendered by the sudden turn to the east of La Perouse bank catalyses a larger
 460 scale instability at this location. Durski and Allen (2005), when modelling the Oregon shelf,
 461 found that including realistic shelf bathymetry catalyzed intermittent large-scale instabilities
 462 similar to the feature here and likely other coastal locations (Battieen, 1997).

463 Large-scale mixing between the shelf and open ocean has been evident since the satellite
 464 era. Here we demonstrate that in the Vancouver Island shelf the flow is originating on the
 465 shelf and separating from the bathymetry and being injected into the interior. A similar
 466 observation was made by Barth et al. (2000) downstream of Cape Blanco, Oregon, where
 467 the coastal current was observed to detach from the shelf in the lee of the cape and flow into
 468 the interior. They hypothesized that as the current moved offshore, it deepened, stretching
 469 isopycnals and creating cyclonic relative vorticity that would tend to push the current back
 470 onshelf, but then it was caught in the undercurrent and stalled, being pushed offshore. It is
 471 also possible that coastally trapped waves in the region experience a hydraulic control, and
 472 these separation events are part of the response (Dale & Barth, 2001).

473 Regardless of the dynamics of the separation events, the offshore transport can be
 474 substantial. If we assume the coastal current is approximately 0.1 m s^{-1} over 100 m in the

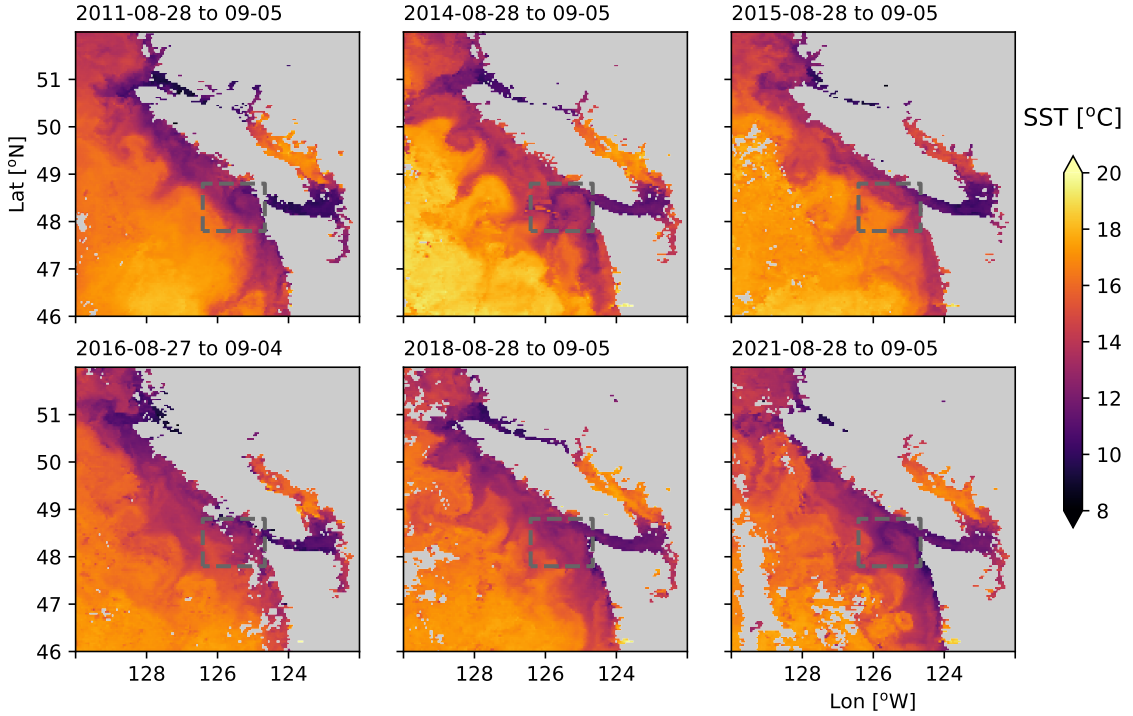


Figure 16. Available late-August sea-surface temperature from 8-day composites, 2011 to 2021 (NASA Ocean Biology Processing Group, 2019); missing years had too much cloud cover or no satellite coverage.

vertical and 20 km in the horizontal, it represents 0.2 Sv of nutrient- and chlorophyll-rich shelf water transported offshore. Our observations are a finer detailed representation of the kind of cross-shore transports inferred by Mackas and Yelland (1999) from hydrographic surveys, and definitively show that this water can originate from the shelf from relatively deep depths and be transported offshore. We do not have velocity measurements for the water that replaces it, but assuming that water also flows along-shelf, these separation events are associated with a large replacement of shelf water with offshore water at this location. This emphasizes the importance of three dimensional observations and modeling of cross-shelf dynamics when thinking about biological processes on the shelf.

484 Open Research

485 Derived data files (1-m vertical binned CTD files) and analysis scripts are available at
 486 <https://ocean-physics.seos.uvic.ca/~jklymak/PW13DataAnalysis/>. Raw CTD data
 487 is available on request. Data was processed using a scientific python toolchain as listed at
 488 <https://ocean-physics.seos.uvic.ca/~jklymak/PW13DataAnalysis/environment.yml>;
 489 major components include xarray (Hoyer & Hamman, 2017), numpy (Harris et al., 2020),
 490 and Matplotlib (Caswell et al., 2022), but those all leverage many smaller but vital projects.

491 Acknowledgments

492
 493 Thank you to the officers and crew of the R/V Falkor and the Schmidt Foundation
 494 for funding the seagoing component of the cruise. Thank you to Richard Dewey, Benjamin
 495 Schieffle, and Rowan Fox for efforts during the cruise. Klymak was supported by Canadian
 496 NSERC grant 327920-2006 and a Canadian Foundation for Innovation Leading Edge Fund
 497 grant 36109.

498 References

- 499 Barth, J. A., Pierce, S. D., & Smith, R. L. (2000). A separating coastal upwelling jet at
 500 Cape Blanco, Oregon and its connection to the California Current system. *Deep Sea*
 501 *Res. II*, 47(5–6), 783 - 810. doi: [http://dx.doi.org/10.1016/S0967-0645\(99\)00127-7](http://dx.doi.org/10.1016/S0967-0645(99)00127-7)
- 502 Batteen, M. L. (1997). Wind-forced modeling studies of currents, meanders, and eddies in
 503 the California Current system. *J. Geophys. Res.*, 102(C1), 985–1010. doi: [10.1029/96jc02803](https://doi.org/10.1029/96jc02803)
- 505 Brink, K. (2016). Cross-shelf exchange. *Annu. Rev. Mar. Sci.*, 8(1), 59–78. doi: [10.1146/annurev-marine-010814-015717](https://doi.org/10.1146/annurev-marine-010814-015717)
- 507 Castelao, R. M., & Barth, J. A. (2007, nov). The role of wind stress curl in jet separation
 508 at a cape. *J. Phys. Oceanogr.*, 37(11), 2652–2671. doi: [10.1175/2007jpo3679.1](https://doi.org/10.1175/2007jpo3679.1)
- 509 Caswell, T. A., Lee, A., Droettboom, M., De Andrade, E. S., Hoffmann, T., Klymak, J.,
 510 ... Kniazev, N. (2022). *matplotlib/matplotlib: Rel: v3.6.0*. Zenodo. Retrieved from
 511 <https://zenodo.org/record/7084615> doi: [10.5281/ZENODO.7084615](https://doi.org/10.5281/ZENODO.7084615)
- 512 Dale, A. C., & Barth, J. A. (2001, jan). The hydraulics of an evolving upwelling jet flowing
 513 around a cape. *Journal of Physical Oceanography*, 31(1), 226–243. doi: [10.1175/1520-0485\(2001\)031<0226:thoaeu>2.0.co;2](https://doi.org/10.1175/1520-0485(2001)031<0226:thoaeu>2.0.co;2)
- 515 Dewey, R. K., & Crawford, W. R. (1988). Bottom stress estimates from vertical dissipation
 516 rate profiles on the continental shelf. *J. Phys. Oceanogr.*, 18, 1167–1177.
- 517 DFO. (2022). *Marine environmental data section archive, buoy c46206*. Ecosystem and
 518 Oceans Science, Department of Fisheries and Oceans Canada. Retrieved 2022-01-31,
 519 from <https://meds-sdmm.dfo-mpo.gc.ca>
- 520 Dortch, Q., Rabalais, N. N., Turner, R. E., & Rowe, G. T. (1994, dec). Respiration rates
 521 and hypoxia on the Louisiana shelf. *Estuaries*, 17(4), 862. doi: [10.2307/1352754](https://doi.org/10.2307/1352754)
- 522 Durski, S. M., & Allen, J. S. (2005). Finite-amplitude evolution of instabilities associated
 523 with the coastal upwelling front. *J. Phys. Oceanogr.*, 35(9), 1606–1628. doi: [10.1175/jpo2762.1](https://doi.org/10.1175/jpo2762.1)
- 525 Engida, Z., Monahan, A., Ianson, D., & Thomson, R. E. (2016). Remote forcing of sub-
 526 surface currents and temperatures near the northern limit of the California Current
 527 system. *J. Geophys. Res.*, 121(10), 7244–7262. doi: [10.1002/2016jc011880](https://doi.org/10.1002/2016jc011880)
- 528 Foreman, M. G. G., Callendar, W., MacFadyen, A., Hickey, B. M., Thomson, R. E., &
 529 Lorenzo, E. D. (2008). Modeling the generation of the Juan de Fuca Eddy. *J. Geophys. Res.*, 113(C3). doi: [10.1029/2006jc004082](https://doi.org/10.1029/2006jc004082)
- 531 Freeland, H., & Denman, K. (1982). A topographically controlled upwelling ceter off
 532 southern Vancouver Island. *J. Mar. Res.*, 40(4), 1069–1093.

- 533 Freeland, H., & McIntosh, P. (1989). The vorticity balance on the southern British Columbia
 534 continental shelf. *Atmosphere–Ocean*, 27(4), 643–657.
- 535 Harris, C. R., Millman, K. J., van der Walt, S. J., Gommers, R., Virtanen, P., Cournapeau,
 536 D., ... Oliphant, T. E. (2020, sep). Array programming with NumPy. *Nature*,
 537 585(7825), 357–362. Retrieved from <https://doi.org/10.1038/s41586-020-2649-2>
 538 doi: 10.1038/s41586-020-2649-2
- 539 Hickey, B., Thomson, R., Yih, H., & LeBlond, P. (1991). Velocity and temperature fluctua-
 540 tions in a buoyancy-driven current off Vancouver Island. *J. Geophys. Res.*, 96(C6),
 541 10,507–10,538.
- 542 Hoyer, S., & Hamman, J. (2017, apr). xarray: N-d labeled arrays and datasets in python.
 543 *Journal of Open Research Software*, 5(1), 10. Retrieved from <https://doi.org/10.5334/jors.148>
 544 doi: 10.5334/jors.148
- 545 Hu, C., Lee, Z., & Franz, B. (2012). Chlorophyll a algorithms for oligotrophic oceans: A
 546 novel approach based on three-band reflectance difference. *J. Geophys. Res.*, 117(C1).
 547 doi: 10.1029/2011jc007395
- 548 Ikeda, M., & Emery, W. J. (1984). A continental shelf upwelling event off Vancouver
 549 Island as revealed by satellite infrared imagery. *J. Mar. Res.*, 42(2), 303–317. doi:
 550 10.1357/002224084788502774
- 551 Ikeda, M., Mysak, L. A., & Emery, W. J. (1984). Observation and modeling of satellite-
 552 sensed meanders and eddies off Vancouver Island. *J. Phys. Oceanogr.*, 14(1), 3–21.
 553 doi: 10.1175/1520-0485(1984)014<0003:oamoss>2.0.co;2
- 554 Klymak, J. M., Shearman, R. K., Gula, J., Lee, C. M., D'Asaro, E. A., Thomas, L. N., ...
 555 others (2016). Submesoscale streamers exchange water on the north wall of the Gulf
 556 Stream. *Geophys. Res. Lett.*. doi: 10.1002/2015GL067152
- 557 MacFadyen, A., & Hickey, B. M. (2010). Generation and evolution of a topographically
 558 linked, mesoscale eddy under steady and variable wind-forcing. *Cont. Shelf Res.*,
 559 30(13), 1387–1402. doi: 10.1016/j.csr.2010.04.001
- 560 Mackas, D. L., Denman, K. L., & Bennett, A. F. (1987). Least squares multiple tracer
 561 analysis of water mass composition. *J. Geophys. Res.*, 92(C3), 2907–2918.
- 562 Mackas, D. L., & Yelland, D. R. (1999, nov). Horizontal flux of nutrients and plankton
 563 across and along the British Columbia continental margin. *Deep Sea Res. II*, 46(11-
 564 12), 2941–2967. doi: 10.1016/s0967-0645(99)00089-2
- 565 NASA Ocean Biology Processing Group. (2017). *MODIS-aqua level 3 mapped chloro-*
 566 *phyll data version r2018.0*. NASA Ocean Biology DAAC. Retrieved from <https://oceancolor.gsfc.nasa.gov/data/10.5067/AQUA/MODIS/L3M/CHL/2018>
 567 doi: 10.5067/AQUA/MODIS/L3M/CHL/2018
- 568 NASA Ocean Biology Processing Group. (2019). *MODIS-aqua level 3 mapped SST data*
 569 *version r2019.0*. NASA Ocean Biology DAAC. Retrieved from https://oceandata.sci.gsfc.nasa.gov/ob/getfile/AQUA_MODIS
- 570 OSI SAF. (2015). *GHRSST level 2p sub-skin sea surface temperature from the Advanced*
 571 *Very High Resolution Radiometer (AVHRR) on Metop satellites (currently Metop-A)*
 572 *(GDS V2) produced by OSI SAF*. NASA Physical Oceanography DAAC. Retrieved
 573 from https://podaac.jpl.nasa.gov/dataset/AVHRR_SST_METOP_A-OSISAF-L2P-v1.0
 574 doi: 10.5067/GHAMA-2PO02
- 575 Pelland, N. A., Eriksen, C. C., & Lee, C. M. (2013). Subthermocline eddies over the
 576 washington continental slope as observed by seagliders, 2003-09. *J. Phys. Oceanogr.*
 577 doi: 10.1175/JPO-D-12-086.1
- 578 Relvas, P., & Barton, E. D. (2005). A separated jet and coastal counterflow during upwelling
 579 relaxation off Cape São Vicente (Iberian Peninsula). *Cont. Shelf Res.*, 25(1), 29–49.
 580 doi: 10.1016/j.csr.2004.09.006
- 581 Sahu, S., Allen, S. E., Saldías, G. S., Klymak, J. M., & Zhai, L. (2022, mar). Spatial and
 582 temporal origins of the La Perouse low oxygen pool: A combined lagrangian statistical
 583 approach. *J. Geophys. Res.*, 127(3). doi: 10.1029/2021jc018135
- 584 Thomson, R. E., & Gower, J. F. R. (1998, feb). A basin-scale oceanic instability event in
 585 the gulf of alaska. *J. Geophys. Res.*, 103(C2), 3033–3040. doi: 10.1029/97jc03220
- 586

- 588 Thomson, R. E., Hickey, B. M., & LeBlond, P. H. (1989). The Vancouver Island Coastal
589 Current: Fisheries barrier and conduit. In R. J. Beamish & G. A. McFarlane (Eds.),
590 *Effects of ocean variability on recruitment and an evaluation of parameters used in*
591 *stock assessment models*. Fisheries and Oceans Canada.
- 592 Thomson, R. E., & Krassovski, M. V. (2015, dec). Remote alongshore winds drive variability
593 of the California Undercurrent off the British Columbia–Washington coast. *J. Geophys.*
594 *Res.*, 120(12), 8151–8176. doi: 10.1002/2015jc011306
- 595 Weaver, A. J., & Hsieh, W. W. (1987). The influence of buoyancy flux from estuaries
596 on continental shelf circulation. *J. Phys. Oceanogr.*, 17, 2127–2140. doi: 10.1175/
597 1520-0485(1987)017<2127:TIOBFF>2.0.CO;2